Romanian Reports in Physics, Vol. 65, No. 3, P. 681–687, 2013

Dedicated to Professor Valentin I. Vlad's 70th Anniversary

SELECTIVE INFRARED EMITTERS BASED ON SILVER NANOWIRES DEPOSITED ONTO SILICON SUBSTRATE

M.C. LARCIPRETE[1], A. BELARDINI[1], R. LI VOTI[1], G. LEAHU[1], C. SIBILIA[1], M. BERTOLOTTI[1]

[1] Dipartimento di Scienze di Base e Applicate per l'Ingegneria – Sapienza Università di Roma Via A. Scarpa 14, I-00161 Roma, ITALY E-mail: mariacristina.larciprete@uniroma1.it

Received June 12, 2013

Abstract. We investigated the infrared emission of randomly oriented silver nanowires deposited onto silicon substrate. Samples were heated and their temperature evolution was monitored with an infrared camera operating in the long infrared range. Experimental results show that the choice of wire length as well as metal filling factor may affect the resulting infrared emission.

Key words: metal nanowires, selective IR emissivity.

1. INTRODUCTION

Tailoring absorbance and emittance in the infrared (IR) range [1–4] and the thermal tuning of optical properties [5] is becoming a crucial task for sensing, thermophotovoltaics as well as for security applications. Several types of metallic nanowires are currently investigated and employed for different applications ranging from plasmonics [6] to nonlinear optics [7–10] and the manipulation of IR radiation [11], to name some. By definition, metallic nanowires have cross-sectional diameters included between few to hundreds nanometers, while their lengths span from hundreds of nanometres to some hundreds microns. Films composed by metallic nanowires may present peculiar optical properties, such as high optical transmittance in the visible range, while still allowing for good electrical conduction [12–13]. As a consequence, they are suitable for all those applications where transparent electrodes are required and compare to more conventional transparent conductive oxides (TCO) [14].

Metallic nanowires mesh, both randomly or systematically oriented, can be employed to tune the effective optical constants of the resulting film, and get peculiar spectral absorbance properties. In the present work we investigate the reduction of thermal emission in the long wavelength infrared range, 8–12 micron, using randomly oriented silver nanowires films deposited onto silicon substrate. The composed structures were characterized by scanning electron micrography (SEM). Their infrared emission was measured under heating condition using a focal plane array (FPA) infrared camera operating in the long wavelength infrared range.

2. SAMPLE PREPARATION

Samples were prepared using two different suspensions of Ag-nanowires in isopropanol (IPA) (25 mg/ml), purchased from Seashell Technology, differing by both nanowires' length and diameter. The geometrical parameters of the nanowires are summarized in Table 1. A small amount of the starting IPA dispersion, corresponding to approximately 0.1 ml, was added to either 50 or 100 ml of de-ionized water. Then, the Ag-nanowires in suspensions were ultrasonicated for few minutes, filtrated and transferred onto a silicon substrate by drop casting.

Table 1

Geometrical parameters and filling factor of the Ag nanowires films

Sample	Diameter [nm]	Length [μm]	Filling factor
NW1	100-130	20-50	~0.04
NW2	100-130	20-50	~0.10
NW3	50-70	5-15	~0.19
NW4	50-70	5-15	~0.30

After film deposition, samples were investigated by scanning electron micrography (SEM), thus quantitative characterization of the resulting metal content in the final film was performed by analyzing the SEM images with a matlab software based on visual method: the software acquires SEM images, whereas each pixel corresponds to an intensity value. Very different intensity values hold for either nanowire (high value) or silicon substrate background (low value), respectively, thus the silver to background fraction can be retrieved. In Fig. 1 we show a scanning electron micrograph image obtained from one of the fabricated films.

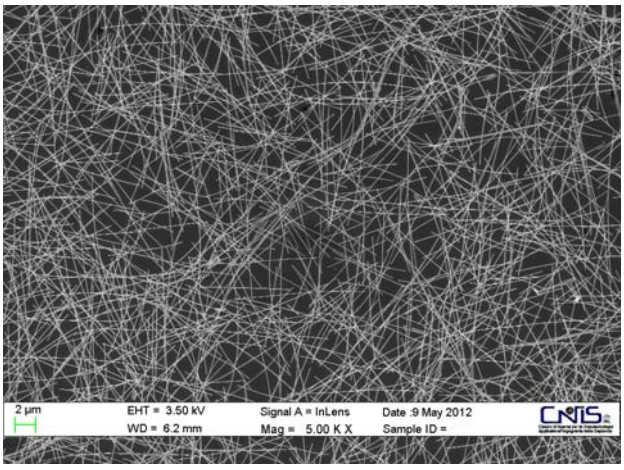

Fig. 1 – Scanning electron micrographs of short type silver nanowires film NW2, deposited onto silicon substrat.

3. IR CHARACTERIZATION

The amount of infrared radiation emitted by the metallic meshes under heating conditions was measured using a calibrated IR-camera (*i.e.* radiometric camera) and compared to the infrared emission of the bare heat source.

Samples were placed onto a hotplate holder, acting as the heat source, allowing maximum heating temperature +200 °C with fast heating-up by powerful integrated electrical heater, homogenous temperature distribution and over-temperature protection inside the plate. Setting the temperature of the integrated heater was allowed through an analog display, with a resolution of ~10°C. Once the hotplate temperature is fixed with this resolution, its actual temperature is accurately read by the IR camera, which is described in the following. Oscillation of the heating current was avoided using a stabilized power supply.

A radiometric forward looking infrared camera (FLIR) operating in the long wavelength infrared range was used to measure the amount of infrared radiation emitted by the nanowires samples, providing detailed images of their apparent temperature. The FPA sensor of this radiometric imaging system is basically a grid of 320×256 pixels, each of them being a vanadium oxide (VOx) uncooled microbolometer integrating the IR signal between 8 and 12 microns, with a characteristic pixel size of 25μm (pitch) and a noise equivalent temperature difference (NETD) of 80 mK. In order to prevent detector saturation, the temperature of sample holder was never exceeding 90°C. The temporal evolution of both heating and cooling processes was systematically monitored by recording a sequence of consecutive infrared images, with a time step of 60 seconds. During imaging recording, samples were kept in direct contact with the heating holder, with wires' coatings facing the infrared camera, in order to avoid film deterioration. Spurious signals arising for thermal reflection generated on the sample surface by external environmental sources was avoided by protecting the camera/sample setup with black opaque shields, thus confining the complete camera field of view (FOV).

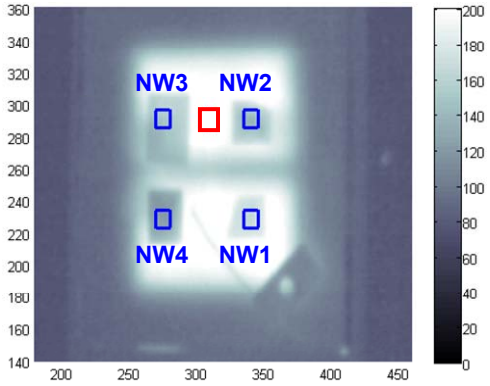

Fig. 2 – Infrared image recorded with a long wavelength IR camera at heating temperature of about 50°C. The four different samples are evidenced with the blue rectangles, while red rectangle holds for the background heated surface, taken as reference.

An example of a typical radiometric image, where the four Ag-nanowires samples are observed in the meantime, and the background heated surface is taken

as a reference, is shown in Fig. 2. This image was recorded at the fixed temperature of ~50°C. The different samples are evidenced with coloured rectangles, while further details can be found within figure's caption. The colorbar at the right side quantifies the amount of IR radiation reaching the camera's microbolometers, in other words the infrared signal integrated between 8 and 12 microns. It can be easily recognized that the intensity level corresponding to the nanowires samples, namely NW1, NW2, NW3 and NW4, appear to be considerably darker, with respect to the intensity level arising form the heating substrate, *i.e.* despite the temperature rise, the infrared images of Ag nanowires films only display a weak bleaching, with respect to the underlying hotplate.

The set of consecutive radiometric images was then examined by means of a MatLab software, thus the IR signal values were retrieved from the images data. For each sample an uniform area was selected over the radiometric images (blue rectangles in Fig. 2) and those data arising from the corresponding pixels were numerically integrated so to obtain the mean value of the resulting IR intensity level, which also corresponds to the resulting apparent temperature. The obtained data are reported in Fig. 3, where the resulting apparent temperature is given as a function of time. According to the temperature values reported for the heating holder, samples were heated during the first ten minutes, then the temperature was kept constant for about thirty minutes, and afterwards the current was switched off to observe the cooling phase.

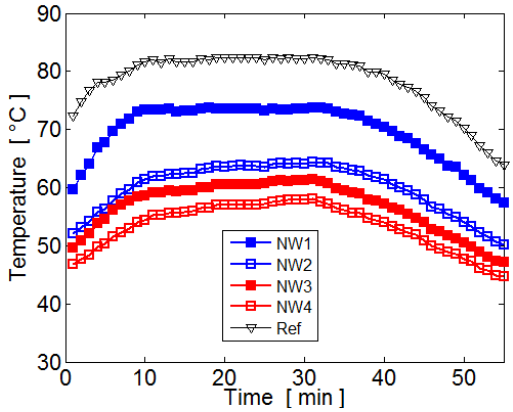

Fig. 3 – Experimental plot of temperature evolution as a function of time, measured in the LWIR range, *i.e.* 8-12 micron for the four different silver nanowires samples (Table 1), during heating and cooling process. The heater was switched off at $t = 30$ min.

The experimental curves show that under heating conditions of about 85°C, the apparent temperature of the nanowires films show a temporal trend similar to the corresponding heating holder temperature, having all curves the same shape. On the other hand, considering their absolute values, the apparent temperature of the four nanowires samples keeps always below that of the heat source, although with some differences among them. In particular, samples pertaining higher metal filling factor display better IR shielding behaviour, *i.e.* samples NW3 and NW4 keep the lower apparent temperatures while NW1 and NW2 stay somewhat higher.

4. RESULTS

The different values of the experimental curves can be interpreted by retrieving the permittivity corresponding to the different nanowires film. Considering an effective medium composed by metallic nanowires randomly aligned in the xy plane, its permittivity has a dyadic form, where $\varepsilon_{xx}=\varepsilon_{yy}$ refer to the plane of the wires and ε_{zz} is in the direction perpendicular to film surface. The relative permittivity of such an effective medium can be calculated by using the mixing formulas for randomly orientated ellipsoidal inclusions reported in [16], as a function of the metal filling factor, *f*. As shown in [11] the transverse, $\varepsilon_{xx}=\varepsilon_{yy}$, and the perpendicular dyadic components, ε_{zz} can be written in terms of the relative permittivities of the host matrix and the wires, respectively.

We here consider a medium composed of air-surrounded nanowires, thus the host matrix permittivity is real and equal to one, while the optical constants of silver were taken from [17]. The metal filling factor *f* is defined as $f = \text{area}_{Ag}/\text{area}_{air}$, where the area of silver or air was thereby evaluated from SEM top-view images by means of their colour contrast.

Since the radiometric emission was detected at normal incidence, *i.e.* perpendicularly to films' surface, we assume that the radiation polarization is equally distributed along the xy plane. Following these considerations, the real and imaginary part of the permittivity components, $\varepsilon_{xx}=\varepsilon_{yy}$, were calculated for the four different silver nanowires meshes in the whole IR investigated range. Next, the refractive index and extinction coefficients were retrieved for the silver nanowires systems, being $\text{Re}(\varepsilon)=n^2-k^2$ and $\text{Im}(\varepsilon)=2n\cdot k$, and used to recover the spectral absorbance *A* from Kirchhoff's law $A=1-|T|^2-|R|^2$, where *T* is the transmission coefficient and *R* is the reflection coefficient *R*, obtained by applying the transfer matrix method.

In Figure 4 these results are summarized for the four different films, whose thickness is assumed to be proportional to wires' diameter. It's worth to note that the optical constants of silicon substrate were also taken into account. It is notable that the combination of different thickness and filling factor may produce different absorbance dispersions, which in turns result in a different trend of the experimental curves. In particular, we note that sample NW4, having the highest metal content ($f = 0.30$) presents the lower absorbance values within the whole investigated wavelength range, since metals behave - in the IR - as a mirror. On the other hand, the sample NW1, due to the lower filling factor ($f = 0.04$), shows a higher absorbance amount, thus experimental data show that it is unable to shield the substrate emissivity.

Both experimental results and theoretical studies reflect the fact that metals in general have very high reflectance values in the IR range. As a consequence, for a metal-based film, the higher the metal content, in terms of either thickness or filling factor, the lower the absorbance in the IR range. In other words, as the film metal content increases, its dielectric constant value becomes closer to that of pure silver, and its IR shielding effectiveness increases.

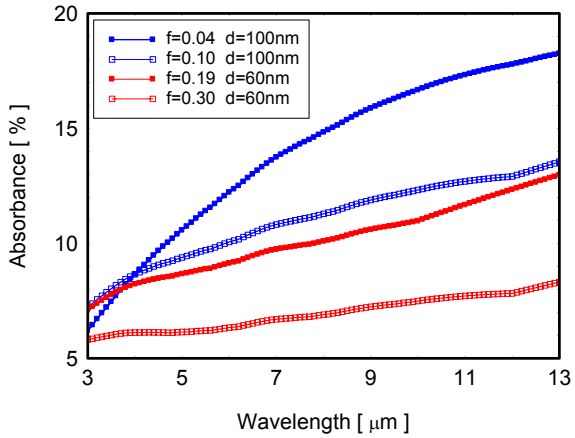

Fig. 4 – Plot of the calculated absorbance spectra using refractive index and extinction coefficient, for the four nanowires' samples, whose data are reported in Table 1. For all calculated curves, the substrate is Si.

5. CONCLUSIONS

In conclusions, we investigated randomly oriented silver nanowires films deposited onto silicon substrates in order to characterize their IR emission under heating conditions in the wavelength range 8-12 microns. This study was performed over a set of films differing in both metallic nanowires' dimensions, length and diameter, as well as metal content. Samples' temperature evolution was observed using a focal plane array (FPA) infrared camera and it was found that silver nanowires films display an apparent temperature which is always below that of the driving heat source. The different experimental curves were interpreted in terms of different absorbance spectra of films, derived from effective permittivity calculations, as a function of metal filling factor in the corresponding film. The obtained results indicate that randomly oriented silver nanowires meshes allow the thermal camouflage of the underlying heat source, even if in direct contact. This opens the way to possible applications of silver nanowires as efficient IR shielding coatings and glaze. The apparent temperature read by the IR camera can also be intentionally heterogeneous, *i.e.* by modifying wires concentration of the starting solution in order to prepare different areas with variable metal filling factor.

***Acknowledgements*.** This work has been performed in the framework of the project "FISEDA" granted by the Italian Ministry of Defence.

REFERENCES

1. N. Mattiucci, G. D' Aguanno, A. Alù, C. Agryropoulos, J. V. Foreman and M. J. Bloemer, *Taming the thermal emissivity of metals: a metamaterial approach*, Applied Physics Letters, **100**, 201109 (2012).
2. R. Li Voti, M.C. Larciprete, G. Leahu, C. Sibilia, M. Bertolotti, *Optimization of thermochromic VO2 based structures with tunable thermal emissivity*, Journal of Applied Physics, **112**, 034305 (2012).

3. R. Li Voti, M.C. Larciprete, G. Leahu, C. Sibilia, M. Bertolotti, *Optical response of multilayer thermochromic VO_2-based structures*, Journal of Nanophotonics, **6**, 061601 (2012).
4. G. D'Aguanno, M.C. Larciprete, N. Mattiucci, A. Belardini, M.J. Bloemer, E. Fazio, O. Buganov, M. Centini and C. Sibilia, *Experimental study of Bloch vector analysis in nonlinear, finite, dissipative systems*, Phys. Rev. A, **81**, 013834 (2010).
5. M.C. Larciprete, C. Sibilia, S. Paoloni, G. Leahu, R. Li Voti, M. Bertolotti, M. Scalora, K. Panajotov, *Thermally induced transmission variations in ZnSe/MgF_2 photonic band gap structures*, Journal of Applied Physics, **92**, 2251–2255 (2002).
6. Y. Sun, *Silver nanowires-unique templates for functional nanostructures*, Nanoscale, **2**, 1626 (2010).
7. A. Belardini, M.C. Larciprete, M. Centini, E. Fazio, C. Sibilia, D. Chiappe, C. Martella, A. Toma, M. Giordano, F. Buatier de Mongeot, *Circular Dichroism in the Optical Second Harmonic Emission of Curved Gold Metal Nanowires*, Physical Review Letters, **107**, 257401 (2011).
8. A. Belardini, M.C. Larciprete, M. Centini, E. Fazio, C. Sibilia, M. Bertolotti, A. Toma, D. Chiappe, F.B. De Mongeot, *Tailored second harmonic generation from self-organized metal nano-wires arrays*, Optics Express, **17**, 3603–3609 (2009).
9. A. Belardini, F. Pannone, G. Leahu, M. C. Larciprete, M. Centini, C. Sibilia, C. Martella, M. Giordano, D. Chiappe, and F. Buatier de Mongeot, *Evidence of anomalous refraction of self-assembled curved gold nanowires*, Appl. Phys. Lett., **100**, 251109 (2012).
10. A. Belardini, F. Pannone, G. Leahu, M. C. Larciprete, M. Centini, C. Sibilia, C. Martella, M. Giordano, D. Chiappe, F. Buatier de Mongeot, *Asymmetric transmission and anomalous refraction in metal nanowires metasurface*, J. Europ. Opt. Soc. Rap. Public., **7**, 12051(2012).
11. M.C. Larciprete, A. Albertoni, A. Belardini, G. Leahu, R. Li Voti, F. Mura, C. Sibilia, I. Nefedov, I. V. Anoshkin, E. I. Kauppinen and A. G. Nasibulin, *Infrared properties of randomly oriented silver nanowires*, J. Appl. Phys., **112**, 083503 (2012).
12. J.Y. Lee, S.T. Connor, Y. Cui and P.Peumans, *Solution-processed metal nanowire mesh transparent electrodes*, Nano Letters, **8**, 689 (2008).
13. A. Madaria, A. Kumar, F. N. Ishikawa and C. Zhou, *Uniform, highly conductive, and patterned transparent films of a percolating silver nanowire network on rigid and flexible sustrates using a dry transfer techinque*, Nano Res., **3**, 564 (2010).
14. F. Michelotti, A. Belardini, M.C. Larciprete, M. Bertolotti, A. Rousseau, A. Ratsimihety, G. Schoer, and J. Mueller, *Measurement of the electro-optic properties of poled polymers at λ = 1.55 μm by means of sandwich structures with zinc oxide transparent electrode*, Appl. Phys. Lett., **83**, 4477 (2003).
15. F. Toschi, S. Orlanducci, V. Guglielmotti, I. Cianchetta, C. Magni, M. L. Terranova, M. Pasquali, E. Tamburri, R. Matassa, and M. Rossi, *Hybrid C-nanotubes/Si 3D nanostructures by one-step growth in a dual-plasma reactor*, Chem. Phys. Lett., **539–540**, 94–101 (2012).
16. A.H. Sihvola, in *Electromagnetic Mixing Formulas and Applications*, Electromagnetic Wave Series, edited by The Institution of Electrical Engineers (IEE Publishing), London, 1999.
17. E.D. Palik, *Handbook of optical constants of solids*, *Subpart 1: Metals*, Academic Press, 1985.